Preprints (www.preprints.org) | NOT PEER-REVIEWED | Posted: 3 January 2019 doi:10.20944/preprints201901.0015.v1

Peer-reviewed version available at Materials 2019, 12, 478; doi:10.3390/ma12030478

Article

Evaluation of Reliefs' Properties on Design of Thermoformed Packaging Using FDM Moulds

Lucía Rodríguez-Parada*, Pedro F. Mayuet and Antonio J. Gámez

Department of Mechanical Engineering & Industrial Design, Faculty of Engineering, University of Cadiz, Av. Universidad de Cádiz 10, E-11519 Puerto Real-Cadiz, Spain; pedro.mayuet@uca.es (P.F.M.A.); antoniojuan.gamez@uca.es (A.J.G.)

* Correspondence: lucia.rodriguez@uca.es (L.R.-P.); Tel.: +34 956 483497 (L.R.-P.)

Abstract: The increased consumption of food requiring thermoformed packaging means that the packaging industry demands customized solutions in terms of shapes and sizes to make the packaging unique. In particular, the food industry increasingly requires more transparent packaging, with greater clarity and a better presentation of the product features they contain. However, in turn, the differentiation of products is sought through the geometry and final finish of the product, as well as the arrangement of food inside the packaging. In addition, these types of packaging usually include ribs in the walls to improve physical properties, however they also affect the final aesthetics of the product. In accordance with this, this research study analyses by studying the mechanical properties of different relief geometries that can affect not only the aesthetics but also their strength. For this purpose, tensile and compression tests have been carried out. The results provide comparative data on the reliefs studied and show that there are different shapes, sizes and layout.

Keywords: packaging design; product design; mechanical properties, thermoforming, tensile test, 3D printing, simulation

1. Introduction

Thermoformed food packaging usually called rigid or semi-rigid containers have as main functions, as in other types of packages, the protection, containment, preservation and distribution [1, 2]. According to this, different types of thermoformed packaging can be observed in the market according to the specific needs of the food. These include heat-sealable containers for processed or semi-processed products [3, 4]; and packaging usually applied to fresh products, such as fruit or vegetables [5], all of which are therefore often used for products with a short life cycle and with the aim of protecting and making food more functional [6]. For this reason, during the development of these containers, the aim is to reduce the amount of material used to increase sustainability by reducing the large amount of waste generated [7]; and also to optimise production costs while maintaining their functional properties [5].

On the other hand, although distribution is one of the main functions [8, 9], most of these packages reach the consumer, especially because of the new trend of food on the move [10]. For this reason the design and finish of these packages must also be taken into consideration. Thus, the ergonomic and functional aspects of the packaging must be aimed at adapting the product to the consumer's needs for use and protection of the food it contains [2].

Throughout the short life cycle of freshly packaged food there are very different situations to which the packaging is exposed to aggressions. This is linked to the sustainability of both the product inside and the cost of material involved. Thus, food packaging can delay and protect food from physical, chemical and biological spoilage, i.e. packaging can extend shelf life and ensure product quality [7]. Light, humidity, microorganisms, shocks and mechanical forces are examples of some of the external agents that can adversely affect food [2]. In general, both the handling of the package, its transport or its stacking on the supermarket shelf are considered external aggressions to the food

© 2019 by the author(s). Distributed under a Creative Commons CC BY license.

Preprints (www.preprints.org) | NOT PEER-REVIEWED | Posted: 3 January 2019 doi:10.20944/preprints201901.0015.v1

Peer-reviewed version available at Materials 2019, 12, 478; doi:10.3390/ma12030478

contained inside before consumption [5]. Based on the above observations, it may be considered necessary for this kind of packaging to have elastic deformation in order not to break with the different situations in which it may be found.

Concretely, the weight of the food generates tensile stresses in the walls. One of the situations in which this occurs is when the container is suspended during transport or handling. Also, during transport the containers are normally also stacked and this means that the container must also withstand the stacking weight. These mechanical forces cause a compressive stress on the container walls. Also, in situations where a user, whether a consumer or not, handles the packaging, a functional situation occurs where the packaging must protect the food [11].

According to these approaches, thermoformed containers usually incorporate patterns on the walls of the container, in the form of relief, which are used to give the container mechanical properties, without the need to increase the thickness of the sheet. In addition, they can attribute a different geometric aspect by creating a semantic value on the product. However, the containers currently used in the market usually only incorporate reliefs in the form of vertical ribs or columns, generally with square geometry.

A related point to consider is the package visual appearance, which influences the decision of consumption due to its symbiotic or simply aesthetic qualities [12, 13]. In these circumstances, the container may be a key factor in the consumer decision-making, allowing inferences to be drawn about the product, its attributes, or its taste. Finally, apart from giving shape to expectations, the package can influence subsequent experiences in the product [14]. So much so that many researchers study its influence in materials, shapes and sizes [3,13-17]. Although a few of them focus on the tactile sensation that the container causes. This is a new trend in packaging, for example in cosmetics or drinks [18]. It can be deduced that a designed texture or relief using differentiating factors can attract consumers as much as shape or colour. Hence, it seems quite interesting the possibility to design custom geometries, although it may alter functional properties.

Given the above conditions, the influence of relief geometries on the mechanical properties of thermoformed sheet is studied and analysed in this work. By means of this methodology, the properties of the reliefs of the packaging can be evaluated in order to guarantee sustainability and also to reduce the expense of plastic material. Furthermore, the improvement of the mechanical properties of the containers also contributes to increase the useful life of the food.

For this purpose, it has been proposed to use Fused Deposition Modelling (FDM), Additive Manufacturing (AM) technology, to make economic moulds that allow thermoforming of test specimens. AM refers as a general term to manufacturing technologies that build up a product layer by layer [19]. Since the 1980´s, AM first started unsteadily and then moved from laboratory to industrial practice. New applications are constantly announced and they develop over time [20]. Thus, the applications of this technology have been increasing. Despite the fact that AM processes, such as Stereolithography (SLA), FDM or Selective Laser Sintering (SLS) were initially created for the purpose of generate rapid prototypes, it is currently sought to use them in order to create final products [21, 22].

In the context of thermoformed products, the findings encountered are research related to creating moulds from additive manufacturing [23]. These applications specifically focus on the study of this technology, in the field of design and development process, in order to create moulds for short series [24]. To do this, additive manufacturing is used to validate proposals as well as for research support, as it allows to generate moulds in a fast and economic way [25, 26].

Nevertheless, it is observed from studies that the investigated technology in the field of thermoforming is the Laser Sintering. In this research, in contrast, the application of the FDM technology is considered since it is an affordable technology and accessible to every design teams [27]. In effect, the creation of moulds by the use of FDM offers the possibility of creating moulds that are suitable for high quality evidence, though it may also result slow and costly [28]. Thus, printers provide the possibility of generating mould in order to create thermoformed prototypes in a rapid way. This results in deadlines being shortened in design development as well as the avoidance of errors.

Preprints (www.preprints.org) | NOT PEER-REVIEWED | Posted: 3 January 2019 doi:10.20944/preprints201901.0015.v1

Peer-reviewed version available at Materials 2019, 12, 478; doi:10.3390/ma12030478

2. Construction of test specimens

In this work a study of the mechanical behaviour of reliefs was carried out. Initially, the reliefs were evaluated as a unit, carrying out tensile tests, with the aim of comparatively analysing the existing differences between geometries and relief sizes. After that, the influence of the positioning and number of the reliefs on the faces of a container, used as a test tube, was studied, performing compression tests.

The overall procedure for the manufacture and preparation of the specimens for the mechanical properties tests consists of several phases, Figure 1: generation of the specimen and mould in CAD using the Solidworks® program, 3D printing of the specimen using Simplify software for the generation of the G-code, thermoforming and cutting of the sheet to obtain the final specimens that will be used for the tests that give rise to the results. For the manufacture of the mould of the specimen printed in FDM is used the 3D printer machine Witbox® and PLA filament with a diameter of 1.75 mm have been used. The machine used for thermoforming the sheet was the table-top thermoforming machine Formech Compac Mini. Finally, Minitab program was used for the treatment of the statistical data.

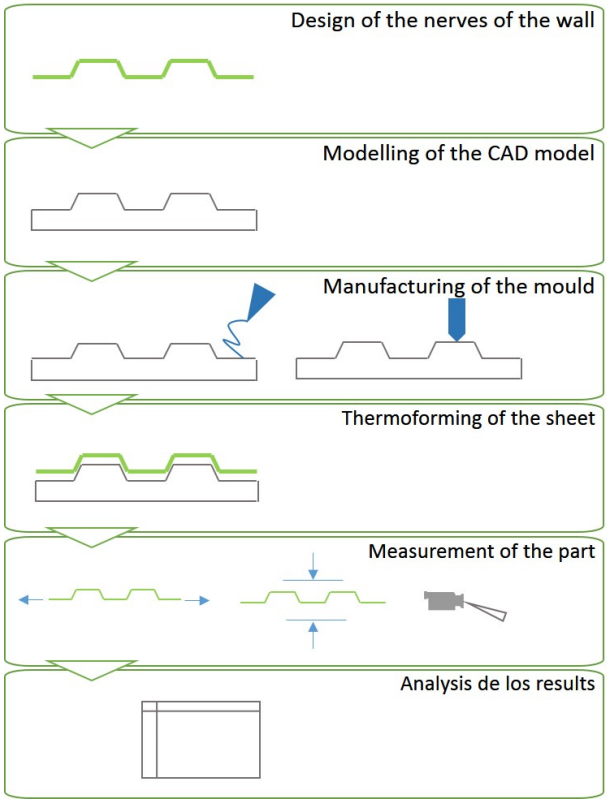

Figure 1. Methodological procedure.

2.1. Procedure for the construction and preparation of tensile specimens.

In the case of the generation of tensile specimens, it is necessary to ensure the flatness on the surface. For this purpose, a two parts hybrid mould was designed, Figure 2 a). One part is common to all the specimens (1), Figure 2 a), and consists of a wooden profile with perforations along the perimeter to ensure that the sheet is fixed along the entire surface during the thermoforming. This profile (1) also serves as a cutting template to remove excess material in order to ensure repeatability during specimen creation. The second part corresponds to the mould of the specific specimen obtained by FDM (2), Figure 2 a), which once printed is fitted into the wooden profile to generate a mould with a flat surface and thermoform the specimen, Figure 2 b). This ensures that there are no rounding along the perimeter of the base of the specimen.

Preprints (www.preprints.org) | NOT PEER-REVIEWED | Posted: 3 January 2019 doi:10.20944/preprints201901.0015.v1

Peer-reviewed version available at *Materials* **2019**, *12*, 478; doi:10.3390/ma12030478

Then, Figure 2 c) shows the procedure for obtaining the final specimen. Once the specimen was thermoformed, the PET sheet is cut. The wooden profile (1) is used to mark the cutting perimeter over the thermoformed sheet. To make the cut, a sheet shear has been used, according to [29].

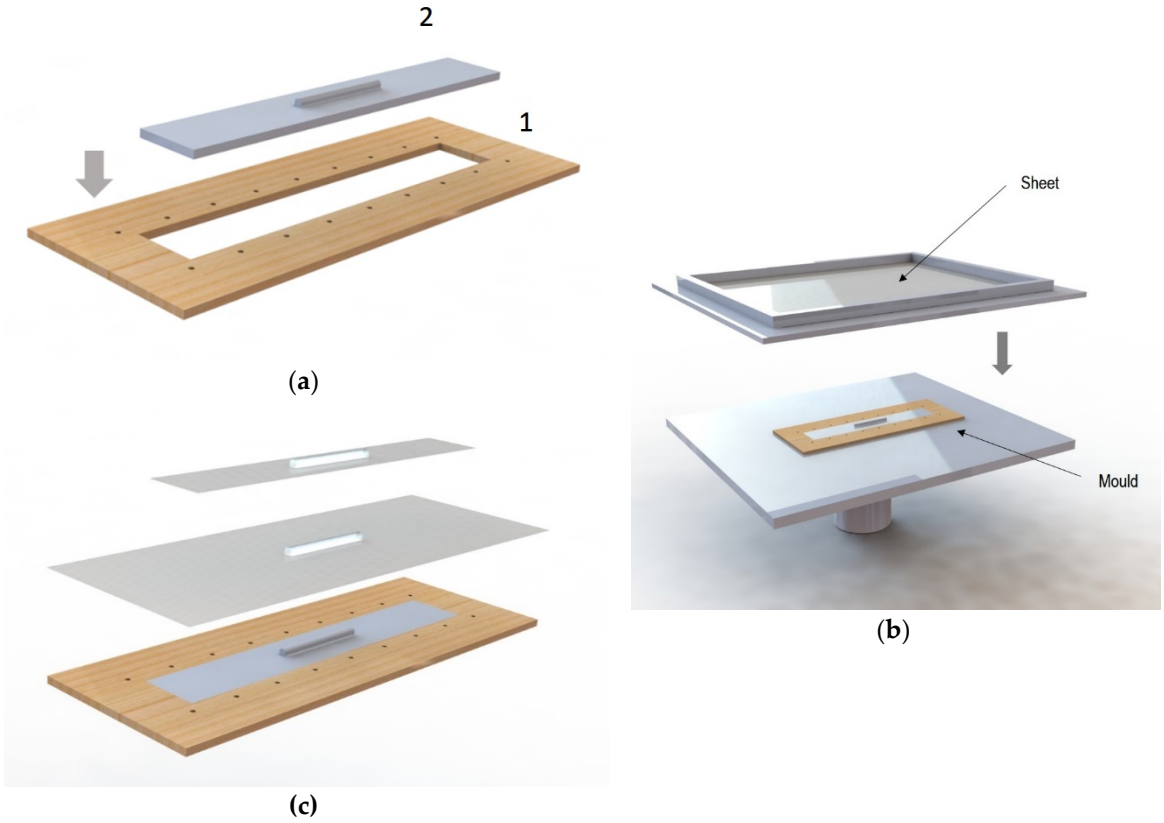

Figure 2. Thermoforming of specimens for tensile tests: a) Hybrid mould; b) Thermoforming of the sheet with hybrid mould to obtain the thermoformed sheet specimen; c) Procedure for obtaining the thermoformed specimen.

2.2. Procedure for the construction and preparation of specimens for compression tests.

The specimens used for compression tests have a square format and a mould made entirely of FDM, Figure 3, is used for their construction. This kind of format is because it has flat sides and this way it can be compared the results with traction.

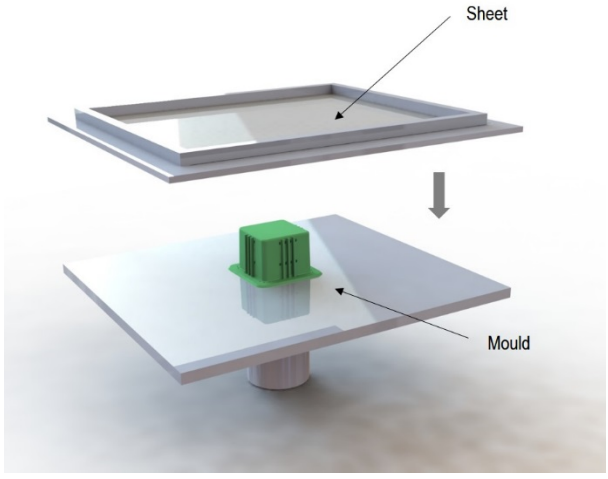

Figure 3. Thermoforming process of specimens for compression tests.

Preprints (www.preprints.org) | NOT PEER-REVIEWED | Posted: 3 January 2019 doi:10.20944/preprints201901.0015.v1

Peer-reviewed version available at Materials 2019, 12, 478; doi:10.3390/ma12030478

The generated mould, Figure 4 a), contains a draft angle and a base with a 45° chamfer to avoid the appearance of defects on the thermoformed sheet, in accordance with [30]. It also contains vacuum channels to ensure proper attachment of the PET sheet to the mould. The channels have been made at 3 heights along the walls of the mould with an angle of 45 °, Figure 4 b).

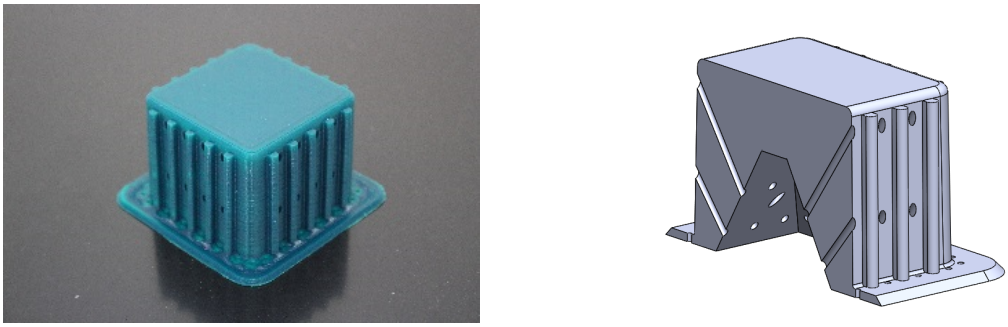

(**a**) (**b**)

Figure 4. Example images of the mould used for thermoforming compression specimens: a) image of the mould, b) vacuum channels included inside the mould.

Once the thermoforming process has been carried out, Figure 3, the excess of the sheet has been eliminated using the Iberolaser IL-1390 laser cutting machine. This cutting procedure is precise and leaves no defects on the cutting surface.

3. Materials and Methods

3.1. Tested material

The material used in this test was a three-layer PET laminate roll with a recycled PET sheet inside and the thickness used was 180 micrometres. The choice of this material is due to the fact that it is the material used for industrial use and is used for food packaging. This material has undergone an extrusion manufacturing process. The properties provided by the supplier are detailed in Table 1, conform to UNE-EN-ISO 527-3 [31] and DIN 53479-B [32].

Table 1. Properties of PET laminate

Thickness	Surface treatment	Tensile strength	Ductility	Impact resistance	Density
0.180 mm ±3%	Silicone on both outer sides	>50 N/mm²	220%	>3 KJ/m²	1.33 gr/cm²

3.2. Tensile test method

The main objective of these tensile tests is to deepen the knowledge of the behaviour of the different geometries in relation to the dimensions of the sheet protrusion. In addition, for the correct evaluation of the reliefs, it is considered necessary to carry out a morphological study of the thermoformed geometries, for this reason the reliefs are included in a unitary way on each specimen.

3.2.1. Morphological study

A total of 9 different types of test tubes were studied based on the study of three different reliefs. On the one hand, three basic geometries were analysed: semicircular (A), square (B) and triangular (C). These geometries are transferred to the PET sheet in a straight line. On the other hand, three size

Preprints (www.preprints.org) | NOT PEER-REVIEWED | Posted: 3 January 2019 doi:10.20944/preprints201901.0015.v1

Peer-reviewed version available at Materials 2019, 12, 478; doi:10.3390/ma12030478

or scale relationships were studied: a, a/2 and 2a where a is 3 mm in the designs made, Figure 5. The value of was selected after analysing the reliefs present in different commercial packages.

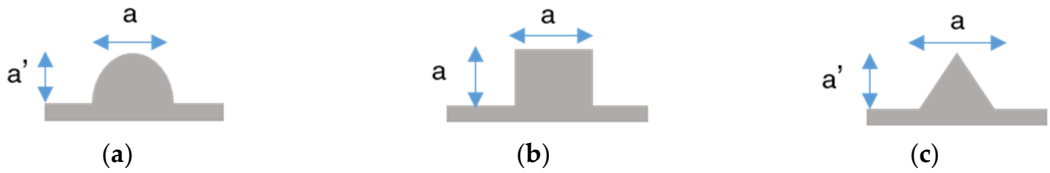

Figure 5. Geometries of the studied reliefs: a) semi-circular; b) square, B.; c) triangular, C.

The different geometries that although sharing the dimensions of height and maximum width do not have the same section area, directly affecting the mechanical properties of the geometry due to the dimensional relationship of equation 1.

$$\sigma = F/A, \quad (1)$$

The area of relief type A presents a semicircular geometry in the upper part and straight sides, the theoretical area of the geometry that is going to be thermoformed is given by equation 2, Figure 6 a).

$$A = (\pi r^2/2) + ab, \quad (2)$$

where a corresponds to the measurement given in the dimensions of the relief and b is the height of the lateral part of the relief.

On the other hand, area type B has rectangular section so the calculation of the area corresponds to equation 3, Figure 6 b).

$$A = ab, \quad (3)$$

Also, the area type C is given by equation 4, corresponding to the area of a triangle according to [30], Figure 6 c).

$$A = ab/2, \quad (4)$$

where a is the width of the triangle, measured by the dimensions of the designed test tubes and b corresponds to the height of the triangle which is the same as a in the mentioned measurement relations.

3.2.2. Mechanical characterization study

In accordance with standard UNE-527-3 [31], Figure 6, in the test specimen designed the dimensions used for b and L3 correspond to 25 mm and 152 mm respectively. As for the relief geometry, included on the flat specimen, the dimensions correspond to the specific ones for each relief geometry, Figure 6. The longitudinal dimension, Lr, remains constant in all the specimens, with a distance of 40 mm. This dimension is less than 50 mm to ensure that the relief studied remains within the test area, L0. Figure 7 shows the types of specimens studied that included the reliefs in the central part.

Preprints (www.preprints.org) | NOT PEER-REVIEWED | Posted: 3 January 2019 doi:10.20944/preprints201901.0015.v1

Peer-reviewed version available at *Materials* **2019**, *12*, 478; doi:10.3390/ma12030478

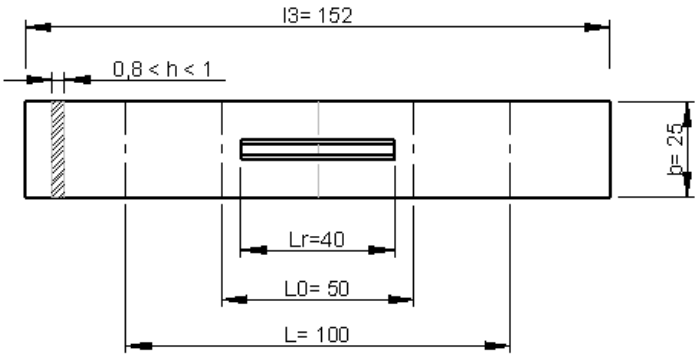

Figure 6. Dimensions of specimen according to standard. Adapted from [31].

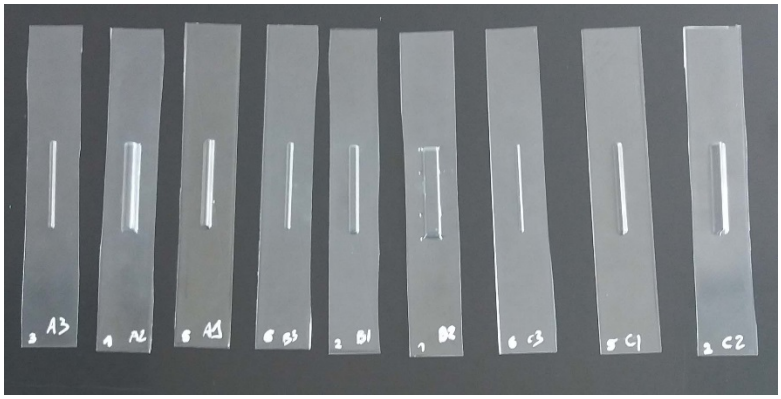

Figure 7. Thermoformed specimens

The guidelines established in [31] y [33] have been taken as a reference for carrying out the tensile tests. Thus, a total of 5 specimens per geometry were studied.

The machine used for mechanical testing is the equipment Shimadzu, model AG-X, with a load cell of 50KN, Figure 8 a). The machine is connected to a desktop computer with which all test parameters are entered by means of the universal test program Trapezium®, which incorporates a user-friendly graphic interface and is compatible with Windows®. For the development of the tests, plastic-specific jaws were used, Figure 8 b).

(**a**) (**b**)

Figure 8. Testing machine with clamps for tensile tests.

Preprints (www.preprints.org) | NOT PEER-REVIEWED | Posted: 3 January 2019 doi:10.20944/preprints201901.0015.v1

Peer-reviewed version available at Materials 2019, 12, 478; doi:10.3390/ma12030478

After the laboratory tests, from which experimental data were extracted, tensile tests were carried out through simulation using a finite element software (FE). The software Solidworks® and Hyperworks® Rasioss were used for geometric modelling and dynamic simulation, respectively.

On the other hand, it is understood that by the properties of the specimens there is the possibility that the results extracted from the simulation can be an approximation to the real tests carried out [34]. In this sense, due to the fact that the greater the range of displacement, the more the test time increases, the study time was defined in 6 seconds. Thus, this range has been able to calculate the behaviour of the specimen including Fy.

3.3. Method for compression tests.

The objective of the compression tests, with a structure similar to that used for tensile tests, is to deepen the knowledge of the behaviour of the reliefs included on the walls of the packaging. The main idea of this study is to evaluate the influence of the number of reliefs on the packaging and the distance between them.

Several reliefs have been introduced on the side and at different distances between them in order to know the influence of the position on the mechanical properties. In this case, the study is restricted to the study of type A geometry (Figure 5a), including the three relief sizes.

3.3.1. Macrogeometric analysis

The moulds and thermoformed packaging have been visually inspected to analyse the final result obtained, Figure 9. Likewise, all the tests carried out have been recorded in order to study the behaviour of the specimens subjected to compression.

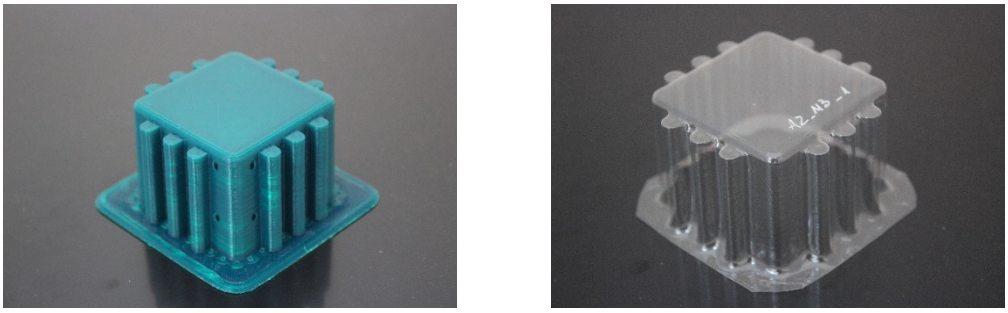

(**a**) (**b**)

Figure 9. Example images of the results obtained: a) mould A2_M3, b) packaging created with mould a).

For the inclusion of the reliefs it was defined to introduce by face: 1, 3 and 5 reliefs. All of them from the centre of the face towards the extremes. In this way the reliefs were placed symmetrically. Table 2 details the photographs of the designed test specimens.

In this sense, two distances between reliefs have been studied: 3 mm and 6 mm. M1 being the test piece that includes 1 relief, M2 and M3 correspond to 3 reliefs, with a distance of 3 and 6 mm respectively, and M4 and M5 correspond to the test pieces that have 5 reliefs, 3 and 6 mm respectively. A2 geometry with 5 reliefs and 6 mm spacing was not evaluated because the size of the specimen face is smaller than necessary to include these reliefs.

Preprints (www.preprints.org) | NOT PEER-REVIEWED | Posted: 3 January 2019 doi:10.20944/preprints201901.0015.v1

Peer-reviewed version available at Materials 2019, 12, 478; doi:10.3390/ma12030478

Table 2. Nomenclature of reliefs according to the type of relief, distance and dimensional correspondence.

Relief	Specimen	Nº reliefs	Relief dimensional proportion	Relief size (mm)	Distance between reliefs (mm)
O2	-	-	-	-	-
A0	M1	1	a/2 x a/2	1.5 x 1.5	-
A0	M2	3	a/2 x a/2	1.5 x 1.5	3
A0	M3	3	a/2 x a/2	1.5 x 1.5	6
A0	M4	5	a/2 x a/2	1.5 x 1.5	3
A0	M5	5	a/2 x a/2	1.5 x 1.5	6
A1	M1	1	a x a	3 x 3	-
A1	M2	3	a x a	3 x 3	3
A1	M3	3	a x a	3 x 3	6
A1	M4	5	a x a	3 x 3	3
A1	M5	5	a x a	3 x 3	6
A2	M1	1	2 a x 2a	6 x 6	-
A2	M2	3	2 a x 2a	6 x 6	3
A2	M3	3	2 a x 2a	6 x 6	6
A2	M4	5	2 a x 2a	6 x 6	3

3.3.2. Mechanical characterization

A total of 15 tests were studied, including the specimen test without reliefs. The geometry of the specimen is of square base and dimensions 50x50 mm, according to [35]. Figure 10 shows an image with the dimensions of the smooth specimen, O2.

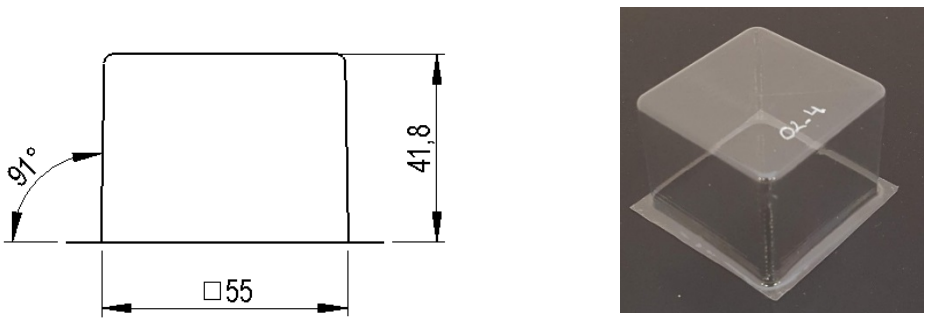

(**a**) (**b**)

Figure 10. Images and dimensions of the plain test specimen, O2: a) general dimensions, b) test specimen.

The compression tests were carried out according to the guidelines established in [35] and [36]. 4 tests were realized per test specimen typology.

The machine used to carry out the mechanical compression tests, Figure 11 a), as well as the tensile tests, Figure 11. The load cell is 50 KN. Like the tensile tests, the test parameters were entered

Preprints (www.preprints.org) | NOT PEER-REVIEWED | Posted: 3 January 2019 doi:10.20944/preprints201901.0015.v1

Peer-reviewed version available at Materials 2019, 12, 478; doi:10.3390/ma12030478

into the software of the Trapezium® equipment. With regard to the compression speed of the tests, the one employed was 10 mm/min, according to [36].

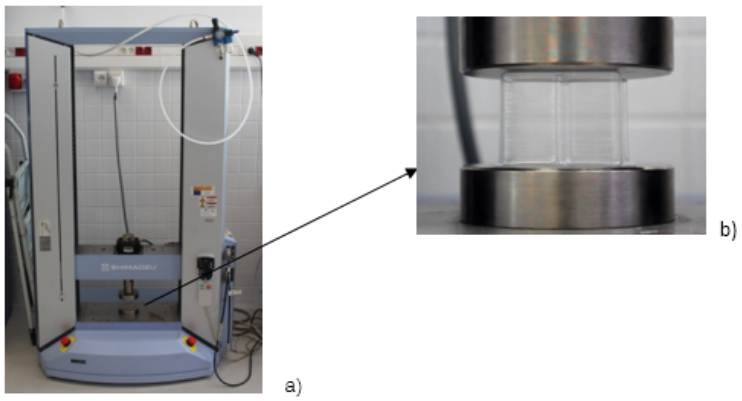

Figure 11. Compression tests: a) general machine view, b) specimen positioning.

The compression tests were recorded using a high-precision digital camera Canon EOS 650D. The recorded images of the compression specimens have been used to evaluate when the containers start to be compressed. In fact, in this experiment it is interesting to observe the deformation with respect to the force that the yield limit; since a container is valid until a deformation that does not affect the product of the interior. In addition, the folds that occur on the walls could generate invalid force data produced by these deformations.

The test procedure started with the placement of the specimens on the cylindrical platform of the testing machine, Figure 11 b). The load cell approaches the specimen and, once the machine has been calibrated, the compression test has begun. The control parameters set in the program were F in N, time in s and displacement in mm.

After carrying out the laboratory tests, a case study was carried out, using the same methodology as in the tensile tests, with one of the test pieces used to compare the simulation with the data obtained in the real tests. This case study seeks to open the line of research on the relationship between the properties of the reliefs on the containers.

The simulation, as in the tensile tests, was carried out with Hyperworks Radioss® and Solidworks® where the base was established as fixed and constant speed was included in the upper side.

4. Results and discussion

4.1.Tensile strength

4.1.1. Mechanical evaluation

As can be seen in Table 3, the three geometries present a different section area produced by the type of relief and size. Thus, the study of thicknesses on the physical specimens was carried out to obtain the real area bearing in mind that the material is stretched where the thermoforming process takes place. According to this, the specimens presented a different tensile strength given by the type of area and volume generated.

Table 3. Results of the area of specimens and tensile strength.

Relieve	Measured section area (mm2)	$\bar{X}$ Fy (N)	Standard deviation
A0	4.60	187.24	15.87
A1	4.82	163.49	22.04
A2	5.31	109.75	15.02
B0	4.68	182.78	22.56

Preprints (www.preprints.org) | NOT PEER-REVIEWED | Posted: 3 January 2019 doi:10.20944/preprints201901.0015.v1

Peer-reviewed version available at Materials 2019, 12, 478; doi:10.3390/ma12030478

B1	4.64	128.53	17.74
B2	5.63	112.71	16.07
C0	4.56	184.06	30.90
C1	4.66	180.38	16.14
C2	4.93	112.84	10.09

As can be seen in Figure 12, geometry 0 provides higher force values compared to the lower ones thrown by geometry 2, independently of the type of form A, B or C. This is related to the fact that a smaller area of section provides a greater wall thickness after thermoforming due to the lower stretching suffered by the specimen and generating greater rigidity to the relief.

Indeed, for this geometry, the smallest, the values reach forces around 185 N, although it is true that it is the A geometry that seems to maintain a lower dispersion in the repetitiveness of the tests. This phenomenon is especially visible in B0 and C0 results, although it is in the latter geometry where there is greater dispersion of the results where some tests reach values of up to 35% lower than the established maximum. This may be due to the fact that the vertices of square and triangular geometry can act as stress concentration points, which can lead to defects and micro-cracks that lead to premature failure.

Geometry 1 presents intermediate force values to those compared for geometry 2 and 0 with greater variability in the averages obtained. Thus, C geometry presents values close to those reached for the smallest relief with an average of approximately 180 N. However, B geometry obtains values closer to those found in higher relief tests with an average of about 130 N. This seems to reinforce what was previously discussed with respect to the area of the section.

In table 3 it can be seen how the section for geometry B1 (4.64 mm2) is considerably higher in proportion to A1 (4.82 mm2) or C1 (4.66 mm2). Thus, it can be established that geometries with a section area less than 5 (A0, B0, C1 and C0) provide higher values of force. As for the dispersion of the results, the tests show similar values independently of the selected shape, although slightly higher in A geometry.

In turn, geometry 2 presents mean values of about 110 N, about 40% lower than the results of geometry 3. In a deeper analysis of the results, the geometry 2 tests show values between 90N and approximately 130 N with smaller dispersions than in previous cases. In table 3 it can be seen how the section for geometry B1 (4.64 mm2) is considerably higher in proportion to A1 (4.82 mm2) or C1 (4.66 mm2). Thus, it can be established that geometries with a section area less than 5 (A0, B0, C1 and C0) provide higher values of force. As for the dispersion of the results, the tests show similar values independently of the selected shape, although slightly higher in A geometry.

In turn, geometry 2 presents mean values of about 110N, about 40% lower than the results of geometry 3. In a deeper analysis of the results, the geometry 2 tests show values between 90 N and approximately 130 N with smaller dispersions than in previous cases.

Thus, the nominal stress analysis shows the trend followed by each A, B and C geometry as a function of their relief. In all three cases there is a tendency for the tension to decrease as the relief increases in size. However, as discussed, the C1 case shows a different trend because its section is proportionally smaller than in cases A1 and B1 and similar to the values obtained in geometry 3.

Preprints (www.preprints.org) | NOT PEER-REVIEWED | Posted: 3 January 2019 doi:10.20944/preprints201901.0015.v1

Peer-reviewed version available at Materials 2019, 12, 478; doi:10.3390/ma12030478

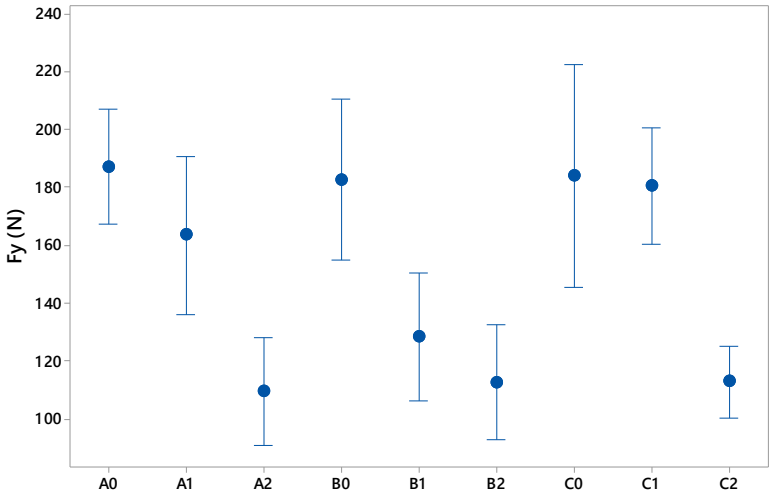

Figure 12. Dispersion of Fy in tensile tests.

4.1.2. Dimensional evaluation

Due to the fact that the base of the specimen influences the result of the tests, the dimensional analysis has been carried out isolating the stress of the relief by means of the dimensional relation given by equation 5:

$$A\ \sigma y\ \text{relief} = \sigma y * \text{Arel}/\text{A}\,, \tag{5}$$

Where A is the real section of area of the specimen, A_b corresponds to real section area of the specimen base and A_{rel} is the real section area of the relief.

Figure 13 details the results obtained according to the middle section, obtaining the tension from the force and area of relief. It is observed that the geometries A1 and C1, which contain the smaller reliefs, support a greater tension, especially C1 in proportion to the relief area. This reinforces the results obtained previously for circular and triangular reliefs with less scale. On the other hand, it can also be seen that the three largest geometries bear less stress, as seen in previous sections, thus highlighting the importance of the relationship between the area of the specimen and the relief.

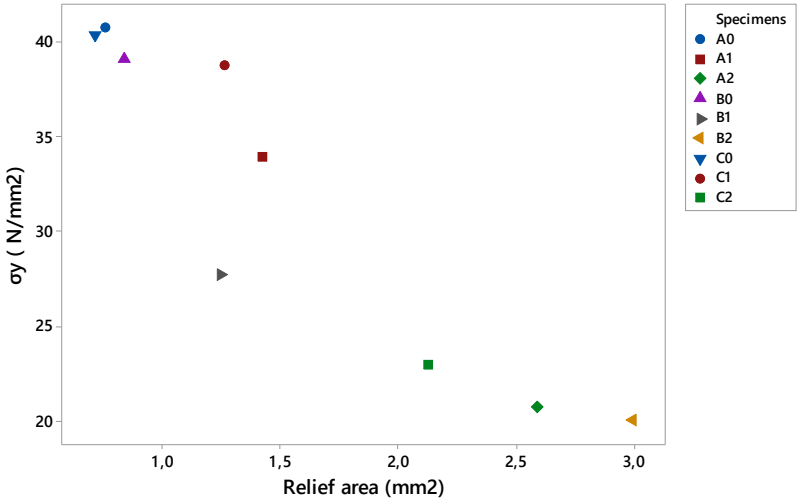

Figure 13. Data of the yield stress with respect to the section area of the relief.

On the other hand, to try to have a detailed view of the results taking into account only the geometry by scale, the dispersion of the results obtained in Figure 14 is shown.

Preprints (www.preprints.org) | NOT PEER-REVIEWED | Posted: 3 January 2019 doi:10.20944/preprints201901.0015.v1

Peer-reviewed version available at Materials 2019, 12, 478; doi:10.3390/ma12030478

Regarding the results for geometry 0, 1.5x1.5 mm, Figure 14 a), it is observed that the differences of Fy are minimal according to relief and size. This may be due to the fact that the area of the relief with respect to the specimen is minimal, and therefore has less influence on the base geometry.

The results of the tests with the specimens with relief geometry 1 of 3x3 mm, Figure 14 b), evidence that there are differences with respect to the dimension of the relief. They also show that C1 geometry withstands the highest stress, and B1 has the lowest tensile strength.

Also, Figure 14 c) shows that the geometries for the largest size studied, relief 2 of 6.5x6.5 mm. Thus, the A2 and B2 reliefs present similar creep stress despite the dimensional differences between them, although the triangular geometry, C2, presents greater strength.

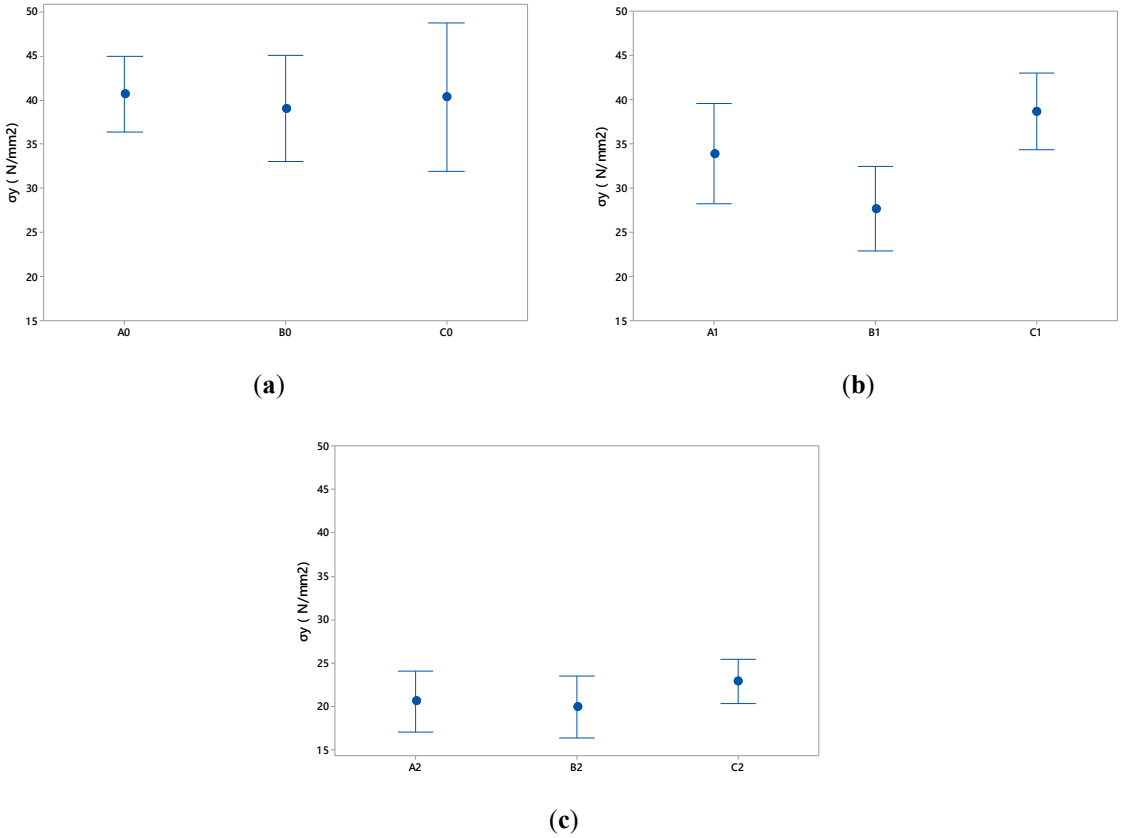

Figure 14. Comparative graph of the average results obtained for the yield stress of the three types of relief (A, B and C): a) for the lower relief measure 0, 1.5x1.5 mm, b) for the lower relief measure 1 of 3x3 mm, c) for the relief measure 2 of 6x6 mm.

4.1.3. Simulation validation

In general, the curve obtained in the different geometries is partially shifted to the left with respect to the experimental ones, probably due to the placement of the specimen in the testing machine, Figure 15. Another explanation can be given by the flexible characteristic of the specimens where the initial tension varies at the beginning of the test. In this way, it is observed that the specimen begins to stress when the jaws move between 0 and 1 mm, i.e., there is a delay that reflects as a consequence the described displacement.

Preprints (www.preprints.org) | NOT PEER-REVIEWED | Posted: 3 January 2019 doi:10.20944/preprints201901.0015.v1

Peer-reviewed version available at Materials 2019, 12, 478; doi:10.3390/ma12030478

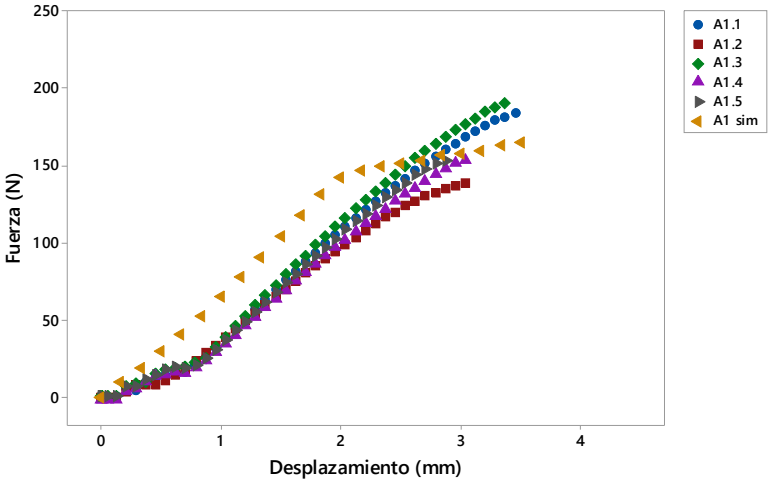

Figure 15. Example graph comparing the results obtained in the simulation test and the experimental studies.

On the other hand, the average values of σy obtained experimentally from the five tests and the values obtained in the simulation are detailed in Figure 16. Thus, and according to [34], it is possible to relate in a comparative way the values obtained in the simulation with respect to the tests using equation 6:

$$Er = \text{Test value-(simulation value)/(test value) x100,} \quad (6)$$

Where Er is the relative error.

In view of the results obtained, it can be considered that the simulation model adequately reproduces the mean specimen rupture with a relative error below 2% for circular and square geometries, and slightly higher for triangular geometry specimens. This may be due to the concentration of stresses in the main corner of the triangular specimen as a consequence of the scale of the meshing and the simplification of the geometries, this being a singular point of study that shows a distorted behaviour in comparison to the rest of the reliefs.

The graph in Figure 16 shows that the C0 and C2 geometries, both with triangular geometry, are the ones with the greatest relative error for the reasons discussed above, although it is the C2 type specimen that lies outside the range of dispersion obtained experimentally, being the only set of tests under these conditions.

It should be noted that for general purposes the simulation results comply to a large extent with the experimental results validating the simulation methodology applied.

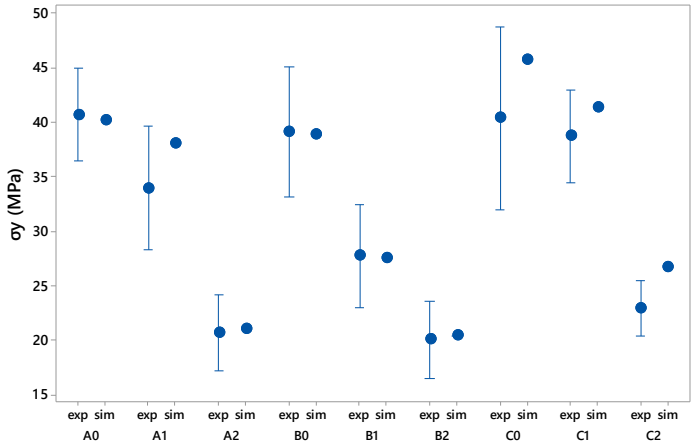

Figure 16. Comparative results of the experimental study (exp) and the simulation carried out (sim) for the yield stress.

Preprints (www.preprints.org) | NOT PEER-REVIEWED | Posted: 3 January 2019 doi:10.20944/preprints201901.0015.v1

Peer-reviewed version available at Materials 2019, 12, 478; doi:10.3390/ma12030478

4.2. Compression tests

4.2.1. Visual Characterization

As it can be seen in the table 4, in general, in the same size of relief the greater the separation of the reliefs, the film adapts better to the contour of the plastic mould. This is due to the stretching of the film. Thus, the lack of definition that occurs when the reliefs are located at a shorter distance can cause the compressive strength of the container to be reduced.

Similarly, the relief size also affects the type of adaptation of the film on the reliefs. Thus, the larger the relief size, the geometry obtained after thermoforming loses definition. According to [37] and [38], this is due to the fact that the machine has to exert greater force to adapt the sheet to the geometry, also producing greater stretching. Thus, in the smaller geometries, A0 and A1, the sheet adapts to the relief, while in the A2 geometry, with a height of 6 mm, in the intermediate spaces between reliefs there is less definition.

It is observed that in the lateral walls the thickness of the sheet is reduced considerably being the part of the sheet where the greatest stretching takes place. Therefore, the smaller the distance between reliefs, the less defined the relief geometry.

Table 4. Kinds of specimens made according to the number of reliefs and disposition.

	M1	M2	M3	M4	M5
A0	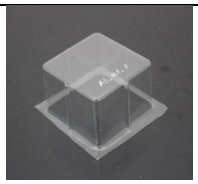	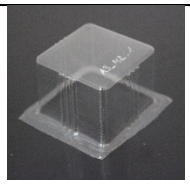	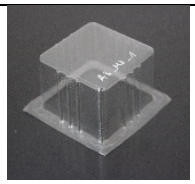	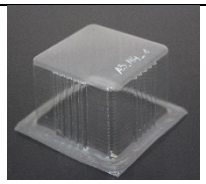	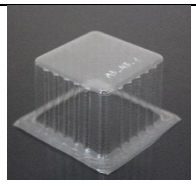
A1	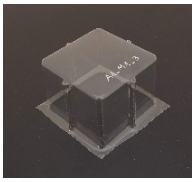	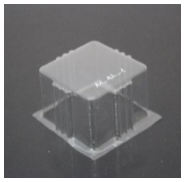	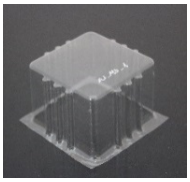	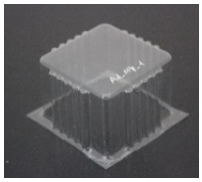	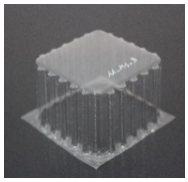
A2	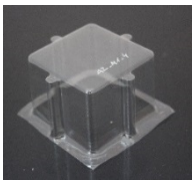	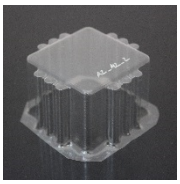	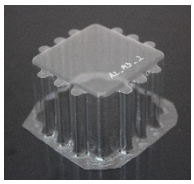	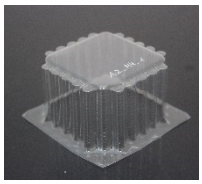	

4.2.2. Mechanical evaluation

The force in the tests made on the thermoformed specimen without reliefs, O2, presents an average Fy of 5.13 N, Figure 17 a). The standard deviation presents an interval amplitude range of 1.18. According to the images collected in the test video, this deviation in the results is due to the fact that the container begins to deform on the walls and folds are produced that could result in different Fy. Thus, it is observed that when there is a displacement of 0.5 mm the container is deformed but no folds are observed. At this moment the average force collected is 3.10 N and deviation of 0.43, Figure 17 b).

From the data collected, it can be seen that the 3 geometries, A0, A1 and A2, improve the F-ε properties with respect to the O2 container, although it is true that A2 shows higher values than the rest. Comparing the results obtained by separation and reliefs, the graph shows that slightly higher results are obtained when the reliefs are arranged with a separation of 6 mm (M3 and M5) conserving the same number of reliefs per face: M3 with respect to M2 and M5 with respect to M4. This phenomenon is in good agreement with the videos studied since the greater the relief, the less the deformation of the walls will be, being able to be due to the fact that a greater distance between reliefs favours that the sheet adapts better to the mould during the thermoforming process.

Preprints (www.preprints.org) | NOT PEER-REVIEWED | Posted: 3 January 2019 doi:10.20944/preprints201901.0015.v1

Peer-reviewed version available at Materials 2019, 12, 478; doi:10.3390/ma12030478

On the other hand, it should be pointed out that although A2 has the highest values of force with respect to A0 and A1, it stands out for reflecting higher deviations, especially in A2-M2 and A2-M3, indicating that the behaviour of these containers is more irregular when tested as a consequence of having a higher relief height.

In Figure 17 b), it is observed that the recorded force data, for a 0.5 mm of displacement, have greater homogeneity when compared at the same point and not at the yield point, where each test shows different values. Thus, in this case, the results show a similar trend in terms of behaviour based on geometry, relief and separation.

In addition, the dispersion of the data is considerably reduced, which indicates that the tests carried out have a greater homogeneity in the first moments of the test and makes it possible to distinguish with greater clarity the package that presents a better relation of properties. And, it should be noted that for deformities greater than 0.5 mm the packaging could lose its functional properties deteriorating the product contained inside.

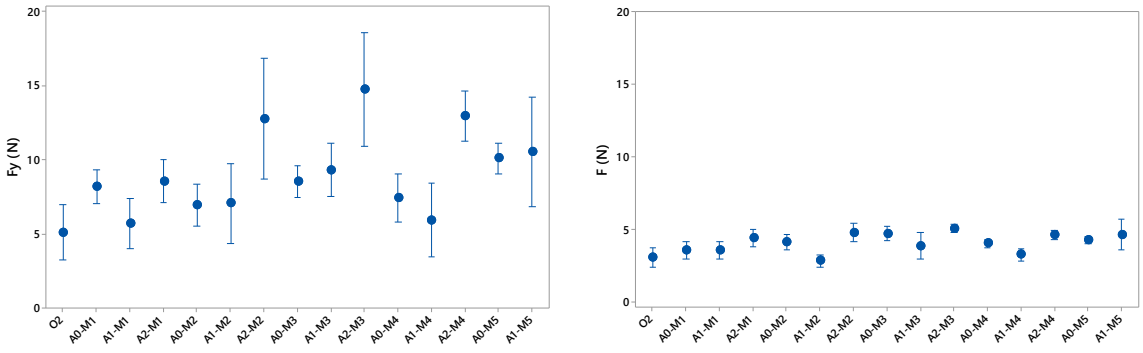

(**a**) (**b**)

Figure 17. a) Compression forces at the moment of stress yield; b) Compression forces when a displacement of 0.5 mm is produced.

4.2.3. Case study of validation by FE.

Figure 18 shows that the compression curve obtained by simulation for the A1-M1 specimen is within the range of experimentally measured values. When a displacement of 0.5 mm occurs, the obtained force data is also homogeneous with respect to laboratory tests.

Thus, the relative error, according to equation 6, is 0.14% with respect to the mean data. It is therefore within the dispersion value collected in the performance of the 4 experimental tests.

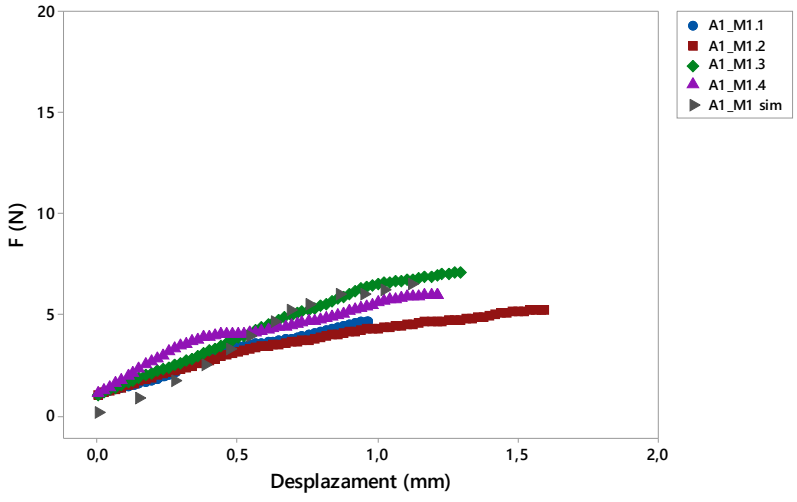

Figure 18. Comparative graph of the results obtained in the compression test by FE.

Preprints (www.preprints.org) | NOT PEER-REVIEWED | Posted: 3 January 2019 doi:10.20944/preprints201901.0015.v1

Peer-reviewed version available at Materials 2019, 12, 478; doi:10.3390/ma12030478

4.3. Relationship between tensile and compressive tests

Figure 19 shows the area graphs that relate the force data obtained in the tensile tests, Fy-T, where the reliefs have been studied in a unitary way, with respect to the results of the compressive strength in two moments, F0.5-C and Fy-C, according to the number of reliefs included per face. Figure 19 a) relates the results of the Fy-T with respect to the force at the moment when the displacement has reached 0.5 mm. On the other hand, in Figure 19 b) the performance is made with respect to the Force to compression at the creep point, Fy-C.

It is observed that the most favourable data of traction and compression, for the force at the moment of 0.5 mm of displacement, are collected with 3 and 5 reliefs per face, Figure 19 a). In the case of the Fy-C, Figure 19 b), the relation of data reflects that the results that obtain an equilibrium of compressive force between 8 and 10 N in addition to good traction results are the containers present 5 reliefs per side.

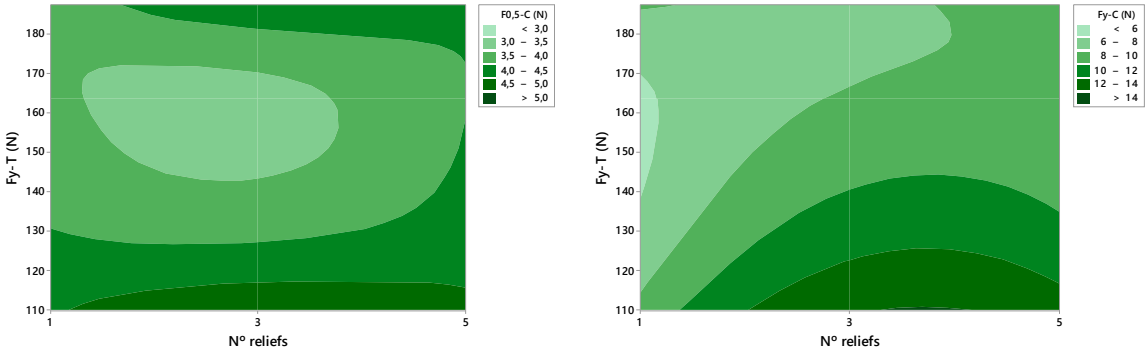

Figure 19. Graph of the Compression Force, F-C, in relation to the number of reliefs per face and the tensile force at the yield point, Fy-T, a) at the moment of displacement of 0.5 mm, F0.5-C, b) at the yield point, Fy-C.

5. Conclusions

The physical tests carried out show that the higher the relief, the lower the tensile strength compared to smaller sizes. This may be due to the stretching of the sheet on the side walls. However, it provides greater rigidity to the container by favouring compressive strength by introducing relief patterns on the surface of the thermoformed container.

From the geometries studied it can be observed that the semi-circular geometry, A, and triangular, C, are the ones that present the best results. And the semi-circular geometry, A, adapts better to the shape of the mould since the shape of the relief has no edges.

Through the analysis carried out, it can be deduced that the main structural factors are the relationship between the width of the relief and its height. In addition, the type of geometry performed affects the mechanical properties. Likewise, from the comparison of the physical tests and the simulation it is concluded that the correct positioning and tension of the specimen on the testing machine influences the displacement registered in the laboratory tests.

Thus, it can be stated that by means of simulation tests a virtual evaluation method can be established as a basis for the optimization of the design applied to thermoformed packaging. In addition, validation by means of FE tests gives rise to the possibility of testing new reliefs with more complex geometries. Therefore, it is proposed that by means of the individualized study of the behaviour of the reliefs it is possible to obtain the behaviour of the relief in order to compare the mechanical properties.

From these studies it is possible to open up a future line of work oriented towards the study of geometric differences on the reliefs usually included in the surfaces of packaging.

On the other hand, it was also possible to develop a methodology that has allowed satisfactory results to be obtained after the compression tests carried out.

Preprints (www.preprints.org) | NOT PEER-REVIEWED | Posted: 3 January 2019 doi:10.20944/preprints201901.0015.v1

Peer-reviewed version available at Materials 2019, 12, 478; doi:10.3390/ma12030478

The results obtained show that the correct design of the reliefs, according to the number of reliefs used and their disposition, can favour the improvement of the mechanical properties of the containers. Specifically, the reliefs with greater distance increase the resistance of the packaging.

Along these lines, a field of study was opened on the inclusion of complex relief patterns on thermoformed surfaces. The realization of complex patterns can be possible by means of the application of thermoformed moulds. Also, these moulds could be used to make cut series and thus improve personalization and brand identity. In short, this work presents a tool for designers that facilitates customization, Ecodesign and allows them to optimize their mechanical properties.

Author Contributions: Conceptualization, L.R.P.; methodology, L.R.P. and P.F.M.A.; software, L.R.P.; validation, L.R.P., P.F.M.A and A.J.G.L.; formal analysis, L.R.P., P.F.M.A and A.J.G.L.; investigation, L.R.P. and P.F.M.A.; resources, A.J.G.L.; data curation, L.R.P., P.F.M.A and A.J.G.L.; writing—original draft preparation, L.R.P.; writing—review and editing, P.F.M.A and A.J.G.L.; supervision, P.F.M.A and A.J.G.L. All authors read and approved the final manuscript.

Funding: The APC was funded by University of Cadiz (Programme for the promotion and encouragement of research and transfer).

Conflicts of Interest: The authors declare no conflict of interest.

References

1. Paine, F.A. *Fundamentals of packaging*. Institute of Packaging, 1981, ISBN 0950756709
2. Trinetta, V. Definition and Function of Food Packaging. *In Reference Module in Food Science*, Elsevier: Amsterdam, Netherlands, 2016. https://doi.org/10.1016/B978-0-08-100596-5.03319-9
3. Hannay, F. *Rigid plastics packaging : materials, processes and applications*. Rapra: Shawbury, UK, 2002, ISBN 1859573584
4. Selke, S.; Culter, J. *Plastics Packaging*, 3rd ed.; Hanser: Munich, Germany, 2016, ISBN 9781569904435
5. Hellström, D.; Olsson, A. *Managing packaging design for sustainable development : a compass for strategic directions*. Wiley: Chichester: Wiley, 2017, ISBN 1119150930
6. Rosato, D.V. Plastics End Use Application Fundamentals. *In: Plastics End Use Applications. Springer Briefs in Materials*. Springer: Berlin, Germany, 2011, pp. 11–18. https://doi.org/10.1007/978-1-4614-0245-9_2
7. Siracusa, V.; Rosa, M.D. Sustainable Packaging. *In Sustainable Food Systems from Agriculture to Industry*, Academic Press: Cambridge, USA, 2018, pp. 275–307. https://doi.org/10.1016/B978-0-12-811935-8.00008-1
8. Baselice, A.; Colantuoni, F.; Lass, D.A.; Nardone, G.; Stasi, A. Trends in EU consumers' attitude towards fresh-cut fruit and vegetables. *Food Qual. Prefer*. **2017**, 59, pp. 87–96. https://doi.org/10.1016/j.foodqual.2017.01.008
9. Cagnon, T.; Méry, A.; Chalier, P.; Guillaume, C.; Gontard, N. Fresh food packaging design: A requirement driven approach applied to strawberries and agro-based materials. *Innov. Food Sci. Emerg. Technol.* **2013**, 20, pp. 288–298. https://doi.org/10.1016/j.ifset.2013.05.009
10. Santeramo, F.G.; Carlucci, D.; De Devitiis, B.; Seccia, A. et al. Emerging trends in European food, diets and food industry. *Food Res. Int*. **2018**, 104, pp. 39–47. https://doi.org/10.1016/J.FOODRES.2017.10.039
11. Simmonds, G.; Spence, C. Thinking inside the box: How seeing products on, or through, the packaging influences consumer perceptions and purchase behaviour. *Food Qual. Prefer.* **2017**, 62, pp. 340–351. https://doi.org/10.1016/j.foodqual.2016.11.010
12. Becker, L.; van Rompay, T.J.L.; Schifferstein, H.N.J.; Galetzka, M. Tough package, strong taste: The influence of packaging design on taste impressions and product evaluations. *Food Qual. Prefer*. **2011**, 22 (1), pp. 17–23. https://doi.org/10.1016/j.foodqual.2010.06.007
13. Westerman, S.J.; Sutherland, E.J.; Gardner, P.H.; Baig, N.; Critchley, C.; et al. The design of consumer packaging: Effects of manipulations of shape, orientation, and alignment of graphical forms on consumers' assessments. *Food Qual. Prefer.* **2013**, 27 (1), pp. 8–17. https://doi.org/10.1016/j.foodqual.2012.05.007
14. Celhay, F.; Boysselle, J.; Cohen, J. Food packages and communication through typeface design: The exoticism of exotypes. *Food Qual. Prefer*.**2015**, 39, pp. 167–175. https://doi.org/10.1016/j.foodqual.2014.07.009
15. Rundh, B. Packaging design: creating competitive advantage with product packaging. *Br. Food J*. **2009**, 111 (9), pp. 988–1002. https://doi.org/10.1108/00070700910992880

Preprints (www.preprints.org) | NOT PEER-REVIEWED | Posted: 3 January 2019 doi:10.20944/preprints201901.0015.v1

Peer-reviewed version available at Materials 2019, 12, 478; doi:10.3390/ma12030478

16. Klimchuk, M.R.; Krasovec, S.A. *Packaging design : successful product branding from concept to shelf*. John Wiley & Sons: Hoboken, USA, 2012, ISBN 1118358546
17. Marcos, B.; Bueno-Ferrer, C.; Fernández, A. Innovations in Packaging of Fermented Food Products. *In Novel food fermentation technologies*, Springer: Cham, Germany, 2016, pp. 311–333. https://doi.org/10.1007/978-3-319-42457-6_15
18. Ritnamkam, S.; Chavalkul, Y. The Design Factors of Cosmetic Packaging Textures for Conveying Feelings. *Asian Soc. Sci*. **2017**, 13 (10), p. 86. https://doi.org/10.5539/ass.v13n10p86
19. Falck, R.; Goushegir, S.M.; dos Santos, J.F.; Amancio-Filho, S.T. AddJoining: A novel additive manufacturing approach for layered metal-polymer hybrid structures. *Mater. Lett.* **2018**, 217, pp. 211–214. https://doi.org/10.1016/j.matlet.2018.01.021
20. Quinlan, H.E.; Hasan, T.; Jaddou, J.; Hart, A.J. Industrial and Consumer Uses of Additive Manufacturing: A Discussion of Capabilities, Trajectories, and Challenges. *J. Ind. Ecol.* **2017**, 21(S1), pp. S15–S20. https://doi.org/10.1111/jiec.12609
21. Collins, P.K.; Leen, R.; Gibson, I. Industry case study: rapid prototype of mountain bike frame section. *Virtual Phys. Prototyp*. **2016**, 11 (4), pp. 295–303. https://doi.org/10.1080/17452759.2016.1222563
22. Ko, H.; Moon, S.K.; Hwang, J. Design for additive manufacturing in customized products. *Int. J. Precis. Eng. Manuf.* **2015**, 16 (11), pp. 2369–2375. https://doi.org/10.1007/s12541-015-0305-9
23. Jiménez, M.; Romero,L.; Domínguez, M.; Espinosa, M.M. Rapid prototyping model for the manufacturing by thermoforming of occlusal splints. *Rapid Prototyp. J.* **2015**, 21 (1), pp. 56–69. https://doi.org/10.1108/RPJ-11-2012-0101
24. Serrano-Mira,J.; Gual-Ortí, J.; Bruscas-Bellido, G.; Abellán-Nebot, V. Use of additive manufacturing to obtain moulds to thermoform tactile graphics for people with visual impairment. *Procedia Manuf.* **2017**, 13, pp. 810–817. https://doi.org/10.1016/J.PROMFG.2017.09.113
25. Boisse, P.; Wang, P.; Hamila, N. Thermoforming simulation of thermoplastic textile composites, 16th European Conference on Composite Materials, Seville, Spain, June 2014, pp. 22-26, ISBN 9780000000002
26. Van Mieghem, B.; Desplentere, F.; Van Bael, A.; Ivens, J. Improvements in thermoforming simulation by use of 3D digital image correlation. *Express Polym. Lett.* **2015**, 9 (2), pp. 119–128. https://doi.org/10.3144/expresspolymlett.2015.13
27. Zhang, Y.; Tong, Y.; Zhou, K. Coloring 3D Printed Surfaces by Thermoforming. *IEEE Trans. Vis. Comput. Graph.* **2017**, 23 (8), pp. 1924–1935. https://doi.org/10.1109/TVCG.2016.2598570
28. Haldane, D.W.; Casarez, C.S.; Karras, J.T.; Lee, J.; Li, C.; et al. Integrated Manufacture of Exoskeletons and Sensing Structures for Folded Millirobots. *J. Mech. Robot.* **2015**, 7 (2), p. 021011. https://doi.org/10.1115/1.4029495
29. ASTM, D 6287-98, Standard practice for cutting film and sheeting test specimens, 1998.
30. Throne, J.L. *Understanding thermoforming*: 2nd ed. Hanser: Ohio, USA, 2008, ISBN 9783446407961. https://doi.org/10.3139/9783446418554.fm
31. UNE-EN ISO 527-3, Determination of tensile properties. Part 3: Test conditions for films and sheets, 1995.
32. DIN 53479, Testing of Plastics and Elastomers; Determination of Density, 1976.
33. ASTM, D 882-18, Standard Test Method for tensile properties of thin plastic sheeting, 2018.
34. Carvalho, C.; Baltar, J. Simulation of uniaxial tensile test through of finite element method. *INOVAE-Journal of Engineering, Architecture and Technology Innovation*. **2017**, 5(2), pp.3-13. ISSN 2357-7797
35. UNE-EN ISO 12048:2001, Pakaging: Comprete, filled transport packages. Compression and stacking test using a compression tester, 2001.
36. UNE-EN ISO 604, Determination of compressive properties, 2003.
37. Loepp, D. Emerging trends in thermoforming. plasticnews, 2015. Available online: http://www.plasticsnews.com/article/20150507/BLOG01/150509942/emerging-trends-in-thermoforming, (accessed on 21 March 2017).
38. Sreedhara, V.S.M.; Mocko, G. Control of thermoforming process parameters to increase quality of surfaces using pin-based tooling. *20th Design for Manufacturing and the Life Cycle Conference,* August 2015, 4, pp. V004T05A016. https://doi.org/10.1115/DETC2015-47682